Zeitschrift für Kristallographie - Crystalline Materials, 2019, V.234, p.513-527DOI: 10.1515/zkri-2018-2152

Phonons in deformable microporous crystalline solids

Bogdan Kuchta[1,2,5], Filip Formalik[1,6], Justyna Rogacka[1], Alexander Neimark[3], Lucyna Firlej[4,5]

[1]Group of Bioprocess and Biomedical Engineering, Faculty of Chemistry, Wroclaw University of Science and Technology, Wroclaw, Poland

[2]MADIREL, CNRS, Aix-Marseille University, Marseille, France

[3]Department of Chemical and Biochemical Engineering, Rutgers University, New Jersey, USA

[4]Laboratoire Charles Coulomb, UMR5221, University of Montpellier - CNRS, Montpellier, France

[5]Department of Physics and Astronomy, University of Missouri, Columbia MO, USA

[6]Department of Theoretical Physics, Faculty of Fundamental Problems of Technology, Wroclaw University of Science and Technology, Wroclaw, Poland

Corresponding author: bogdan.kuchta@univ-amu.fr

Abstract

Phonons are quantum elastic excitations of crystalline solids. Classically, they correspond to the collective vibrations of atoms in ordered periodic structures. They determine the thermodynamic properties of solids and their stability in the case of structural transformations. Here we review for the first time the existing examples of the phonon analysis of adsorption-induced transformations occurring in microporous crystalline materials. We discuss the role of phonons in determining the mechanism of the deformations. We point out that phonon-based methodology may be used as a predictive tool in characterization of flexible microporous structures; therefore, relevant numerical tools must be developed.

Introduction

Many macroscopic properties of solids depend on microscopic lattice mobility, defined as small vibrations of the atoms around their (average) equilibrium position. The collective vibrations of atoms in crystals are called phonons [1]. In stable crystals the amplitude of phonons is small; however, these vibrations are responsible for dynamic lattice deformations whose wavelength is comparable to the interatomic distances. Some solid-state properties (such as heat capacity, thermal expansion, and structural transformations) would not exist if the crystals were absolutely rigid.

In this paper we review the role of phonons in structural transformations occurring in crystalline microporous materials, in particular, those observed during adsorption of guest molecules [2–8]. Although the structural transformations in flexible nanoporous systems have already been summarized in several papers [2–10],the role of the phonons, and in particular, their contribution to the deformation mechanism, has been rarely mentioned [11] and never reviewed. However, phonons are supposed to play an important role in the transformation mechanism, as they represent the lowest energy mechanical fluctuations in the solid state. In consequence, they initiate lattice deformations and define the natural path of structural transformations

An understanding of the microscopic mechanism of adsorption-induced deformations of lattice structure became important with the synthesis of non-rigid metal organic frameworks (MOFs). These functional, third-generation MOFs [3] are often called *soft porous crystals* (SPCs). They show an important flexibility of the structural framework when they are exposed to an external stimulus (light, electric field, variation of thermodynamic parameters, or variation of the pore filling) [12–15].

The observation of the large breathing effect in MOFs [14,16–19] brought about the fascination by the adsorption-induced deformations of the porous structures. The family of MIL-53 breathing MOFs constitutes a prominent example of such SPC systems [4,5], often reviewed from the point of view of the routes of their synthesis and the effects of various functionalities on breathing behaviors [5]. The breathing effect upon adsorption has been also observed in other groups of microporous systems: in MIL-47(V)-type materials (MIL-47, COMOC-2, and COMOC-3) [6], in zeolitic imidazolate frameworks (ZIFs) [7,20] and in DUT materials [9,21–24].

Obviously, lattice flexibility is not restricted to breathing phenomena and phase-transitions involving large changes of the unit cell volume. The so-called gate opening [25], consisting in reorientation of the structure linker which allows the molecules of adsorbent to easy access the pores' interior, has been observed in ZIF-8 material [9]. Another type of transformation consists in structure swelling ($\Delta V \neq 0$), occurring without symmetry change or subnetwork displacements [9].

The crystal-to-crystal structural transformations induced by guest adsorption were first categorized by Kitagawa [2], then the requirements for large unit cell volume change in three-

dimensional, hybrid porous structures were reviewed by Ferey and Serre [4]. Both authors pointed out that the framework flexibility results from the existence of 'weak points' in the structure which allow for low energy deformation of the framework. The effective deformation is a consequence of the competition between guest–guest and host–guest interactions that maintains the system in equilibrium. However, lattice mechanical properties, and, in particular, lattice flexibility are the consequence of the intra-framework (host-host) interactions. The host–guest (and, to some extent, guest-guest) interactions define rather the responsivity of the flexible system to adsorption stimuli.

We focus on the existing examples of applications of phonons for characterization of the crystalline microporous solids and discuss what particular information can be inferred from the phonon spectrum analysis. Finally, we shortly discuss the available methodology and the numerical approaches for the calculations of phonon spectra in porous materials.

Phonons and structural transformation

Correlated atomic vibrations, like phonons (also called normal modes), which represent dynamic mechanical deformations of crystalline structures may in turn induce the structural transformations [26–29]. The transitions may be discontinuous (of the first order) or continuous (of the II order). In general, the phase transition can be driven by different stimuli: thermodynamic (variation of temperature or pressure), adsorption/desorption of individual chemicals (or their mixtures at certain composition), etc. If the driving parameter is temperature, the high-temperature phase is often more disordered and its average observed symmetry is higher than that of the low-temperature phase.

Structural fluctuations in a periodic solid (consisting in correlated deformation of small localized dynamic distortions of the lattice) can be described using a complete set of collective vibrations (phonons). The frequency of such vibrations is determined by the restoring forces acting on atoms fluctuating around their equilibrium positions in the crystal [1,26,29]. The displacement vectors (mathematically called eigenvector) of vibrations determine the polarization (geometrical space orientation) of dynamic deformations. A transition from one crystal structure to another can be totally described in terms of normal modes, geometrically characterized by the displacement polarization vectors. The multidimensional displacement vector of the phonon mode is the set of atomic displacements Δr relative to the initial lattice sites. The restoring forces approaching zero value indicate the appearance of a structural instability of the system. Macroscopically, a transition from elastic dynamic fluctuations Δr ($\langle \Delta r \rangle = 0$) to static deformation ($\langle \Delta r \rangle \neq 0$) is then observed.

In such situation, the simple soft-mode concept may provide the essential characterization of the transformation mechanism. A soft mode is a vibrational mode (phonon) which becomes unstable (its frequency tends to zero) when the system approaches a structural transformation. In general, if a particular normal mode has low energy (frequency), static displacements of the atoms become possible. The structure of the new phase is determined by the polarization vector of the

soft mode, which defines the frozen (static) displacement of the atoms in the new unit cell. When the transformation is driven by variation of temperature, the instability (or so-called softening) of the mode at $T = T_{ph}$ (the temperature of phase transition) is a consequence of the renormalization of phonon frequencies by temperature-dependent anharmonicity of the crystal lattice. It is important to emphasize that the phonon frequency can be altered also by any other external stimuli, such as pressure or adsorption of guest molecules.

The evolution of the phonon spectra is the first indicator of the possible structural transformations of the lattice and may bring the information about its mechanism. In the recent paper [29], we have applied the soft phonon mode analysis to in ZIF-8 type MOFs. The determination of the phonon frequency ω was based on the calculations of the dynamical matrix $D(\boldsymbol{q})$ which depends on coefficients $V_{\alpha\beta}(li, l'j)$, calculated as the second derivatives of the potential energy U. These coefficients are called atomic force constants [1,26]. Mathematically they are referred as the Hessian matrix:

$$\omega^2 u_\alpha(i) = \sum_{\beta,j} D_{\alpha,\beta}(i,j;\boldsymbol{q})\, u_\beta(j)$$

$$D_{\alpha,\beta}(i,j;\boldsymbol{q}) = \frac{1}{\sqrt{m_i m_j}} \sum_{l'} V_{\alpha\beta}(0i, l'j) \mathrm{e}^{-i\boldsymbol{q}\left(\boldsymbol{R}(0)-\boldsymbol{R}(l')\right)}$$

The $\alpha, \beta = x, y, z$ are the Cartesian coordinates. The l, l' and i, j are the indices of lattice unit cells and the atoms in any unit cell, respectively. The wave vector $\boldsymbol{q}$ in the exponent defines the modulation of the phonon amplitude along the periodic lattice. m_i is the mass of an atom i, and $u(i)$ represents its unknown displacement from equilibrium position in the unit cell independent of the index l [29].

The instantaneous position $u_\alpha(l, i)$ ($\alpha = x$,y, or z) of the atom i in the unit cell l corresponding to a phonon ($\boldsymbol{q}, m$) is described by the plane wave functions [1,29]:

$$u_\alpha(l, i) = \frac{1}{\sqrt{m_i}} \sum_{\boldsymbol{q},m} e_\alpha(i, \boldsymbol{q}, m) \mathrm{Q}(\boldsymbol{q}, m) \mathrm{e}^{i\boldsymbol{q}\boldsymbol{R}(l)}$$

The wave-vector $\boldsymbol{q}$ characterizes phonons having different periodicity. The phonons from the center of the Brillouin zone ($\boldsymbol{q} = 0$, so called Γ point in the Brilouin zone, BZ) represent vibrations identical in all unit cells. All other points in the Brillouin zone represent instantaneous deformations of the crystalline lattice having a supercell periodicity. Vector $\boldsymbol{e}(i, \boldsymbol{q}, m)$ represent the polarization of the phonon m with the wave-vector $\boldsymbol{q}$, and $\mathrm{Q}(\boldsymbol{q}, m)$ is its amplitude.

The characteristics of experimentally observed the breathing transformation in MIL-53 depends on the nature of the external stimuli causing the transformation [13,14]. The transition induced by the variation of system temperature is strongly discontinuous, thermodynamically irreversible, and presents a large hysteresis. Starting from the high temperature large pore (LP) open form, upon cooling down the structure transforms into the low temperature narrow pore

(NP) closed form [13]. The phase transition is observed between 150 K and 125 K. With increasing temperature, a large hysteresis is observed, the structure transforms back to the open form between 325 K and 375 K. When the external stimuli consist in adsorption of CO_2 or water, the variation of the adsorbed gas mass upon adsorption/desorption cycles is continuous [19]. At the same time, the structure shows bistability in the hysteresis range [30]. Consequently, the transformation mechanism in those two cases (temperature versus adsorption stimuli) must be of different nature.

When the structural transformation is induced by temperature, the entropic factor promotes the more symmetric open structure. The variation of the temperature modifies the difference between the free energies of open and close pore phases, but their metastable character is conserved. On the other hand, when the transformation is induced by adsorption, the presence of guest molecules modifies the forces acting on the framework atoms and shifts the equilibrium of the framework structure. If the host-guest interactions would be strong enough, the intermediate framework structures (between open and closed pores forms) could be stabilized. It was estimated that an adsorption enthalpy higher than 20 kJ mol^{-1} is required to observe adsorption-induced transition from large to narrow pore structure in the MIL-53(Cr) [30]. In such situation, the minimum of the free energy evolves along a reversible path through a continuum of equilibrium states. However, to the best of our knowledge, there is no experimental observation of such behavior. In particular, in the case of CO_2 adsorption, the hysteresis (due to the structure bistability) is always observed [31].

In principle, the soft phonons should not be observed in the flexible structures exhibiting breathing type transformations, which are generally considered as the first order phase transitions. The breathing transitions exhibit a pronounced first order character and the observed large hysteresis implies that the limiting NP and LP structures may coexist at some thermodynamic conditions (temperature, adsorbate pressure, or external pressure). However, a presence of a soft mode in the MIL-53 materials was suggested by Ghoufi et al. [11]. Using Molecular Dynamics simulations, the authors demonstrated that the host framework transformation occurring during CO_2 adsorption, consists in a progressive dynamic of the deformation rather than a strict transition between two distinct states. They suggested that the host/guest interactions induce a soft mode in the host framework, as a result of the structure reaction to the adsorption stress [23]. They assumed that the appearance of the soft mode occurs at the conditions of the critical threshold adsorption stress exerted by the guest molecules on the framework, at which the framework becomes unstable and keen to the transition from elastic to plastic deformation [32]. Such an interpretation would be an alternative explanation compared to the mechanistic scenario of breathing transition as a nucleation driven shearing of MIL-53 framework [33]. In this content, it is worth noting that the structural transition in MIL-53 materials is associated with a pronounced hysteresis and does not occur at the equilibrium conditions of the phase coexistence, rather at the limit of metastability of the overstretched (NP to LP transition) or overcompressed (LP to NP transition) framework. The question of whether

the metastability limit is associated with the formation of the soft mode is still open and requires further investigation.

In the case of a pore opening type lattice deformation, the rigorous calculations of the phonon energies and symmetry may help to interpret the deformation mechanism and the experimental phonon spectra [29]. In more complex crystals, containing many atoms in the unit cell and, consequently, many phonon vibration frequencies, it might be helpful to know which atom vibrates in a given phonon mode. This information can be extracted from the phonon eigenvectors corresponding to the calculated eigenvalues of frequencies ω.

Phonon calculations: methodology and existing software

As recalled in previous paragraph, calculations of phonon-related properties require an evaluation of *Hessian matrix* which contains second derivatives $V_{\alpha\beta}(li, l'j)$ of the potential energy. There are two ways to calculate the energy of crystalline systems and their derivatives. The first one is based on quantum, *ab-initio* approach; the second uses classical (semi-)empirical force fields approach. In the first case, the most often used method is electronic density functional theory (DFT) which assumes that all properties of a system can be derived from electron density of its ground state [34]. Although the DFT methodology is well defined and presents many advantages, its accuracy depends on the adequate choice of exchange-correlation functional [35]. In the case of deformable structures, where some intermediate configurations may be stabilized by weak van der Waals (dispersion) forces, it is particularly important to include in calculations the corrective terms accounting for dispersion energy. The methodology related to this problem will be discussed latter.

In quantum mechanics calculation of the first derivative of energy E with respect to parameter λ is straightforward from Hellmann-Feynman theorem [36]:

$$\frac{dE}{d\lambda} = \frac{d}{d\lambda}\langle\psi|\widehat{H}|\psi\rangle = \left\langle\frac{d\psi}{d\lambda}\middle|\widehat{H}\middle|\psi\right\rangle + \left\langle\psi\middle|\widehat{H}\middle|\frac{d\psi}{d\lambda}\right\rangle + \left\langle\psi\middle|\frac{d\widehat{H}}{d\lambda}\middle|\psi\right\rangle =$$

$$= E\left\langle\frac{d\psi}{d\lambda}\middle|\psi\right\rangle + E\left\langle\psi\middle|\frac{d\psi}{d\lambda}\right\rangle + \left\langle\psi\middle|\frac{d\widehat{H}}{d\lambda}\middle|\psi\right\rangle =$$

$$= E\frac{d}{d\lambda}\langle\psi|\psi\rangle + \left\langle\psi\middle|\frac{d\widehat{H}}{d\lambda}\middle|\psi\right\rangle,$$

where the Hamiltonian $\widehat{H} = \widehat{T} + V$. As $\langle\psi|\psi\rangle = 1$, $E\frac{d}{d\lambda}\langle\psi|\psi\rangle = 0$. If we set displacement as an independent parameter, $\left\langle\psi\middle|\frac{d\widehat{H}}{du}\middle|\psi\right\rangle = \frac{dV}{du}\langle\psi|\psi\rangle = \frac{dV}{du}$.

The calculation of the second derivative of total energy contains the derivatives of the wave functions that cannot be calculated analytically but may be evaluated explicitly using a

perturbation approach. Finite displacement method (FD) is based on the numerical approximation of a derivative (force F):

$$\frac{d^2E(u)}{du^2} = \frac{dF(u)}{du} \cong \frac{F(u+\Delta u)-F(u-\Delta u)}{2\Delta u},$$

where Δu is the finite displacement of atoms, usually of order of 10^{-2} Å to 10^{-3} Å. The method is relatively robust and can be applied to all types of materials, however, it is naturally constrained to sampling of the Brillouin zone at $q = \Gamma$ of the simulated unit cell. This limitation can be overcome by performing calculation within a supercell. The dynamical properties are then extracted by computing the forces created by the atomic displacements. The supercell approach reduces the accuracy of the calculated phonons. However, (we cite from [37]): *(i) If the interaction range is confined to the supercell interior, then all phonon frequencies are exact. (ii) If the interaction range exceeds the supercell size, then nevertheless there are exact phonon frequencies, which occur for exact discrete wave vectors q. The discrete wave vectors must be commensurate with the supercell size.* The Supercell method is implemented in CASTEP software. It can also be used together with the VASP code if combined with an external code such as phonopy [38] or PHONON [39] which performs a set of single-point DFT calculations and evaluates force constants from the calculated the forces in the supercells. The detailed discussion of the supercell method is well documented in the literature, for both harmonic approximation [40], and anharmonic extension [37].

The two most frequently used approaches to describe electron wave functions within DFT are periodic plane waves functions and localized, Gaussian-based orbitals. The first approximation is implemented in VASP [41–43], CASTEP [44], Quantum ESPRESSO [45], whereas Gaussian orbitals are used in the CRYSTAL package [46]. In what follows we focus on the methodology of the evaluation of the second derivative of the energy (with respect to atoms' displacement) implemented in VASP and CASTEP. Both codes use the finite displacement method (FD) and density functional perturbation theory (DFPT).

DFPT allows one to determine the response of a material to an external perturbation (electric or magnetic field, or atoms displacement), and to calculate the phonons for any wavevector from the Brillouin zone. The extended description of DFTP approach used for phonon calculation can be find in the papers by Gonze et al. [47] (for a perturbation-theory-based approach), and Baroni et al. [48] (for a Green-function-based method). The first method is implemented in VASP; the CASTEP package contains both approaches.

The gradient-based functionals are the most fundamental approximations to describe nanoporous materials. In many benchmarking studies it has been shown that PBE and PBEsol functionals properly describe lattice parameters, bond lengths and angles [49–52], elastic properties and partial charges [53] of MOFs. It has been also shown that long-range interactions resulting from the van der Waals forces are essential to accurately describe stability and structural properties of porous crystals. In soft porous crystals the correct accounting for

dispersion forces allowed to obtain stable materials' conformers, experimentally proven to exist. The addition of the empirical dispersion correction D2 [54] to the PBE functional allowed to obtain a stable, closed-pore form of MIL-53(Al), intermediate between the form of MIL-53(Fe) and the gate-closed form of ZIF-4 [55]. The same effect was also observed for other materials with MIL-53 topology, DUT-8, DUT-49, or COMOC-2. In the collapsed forms of such materials aromatic rings of the linkers are located at a short distance, and the dispersion interactions become strong enough to attract the linkers and close the pore. Besides empirical corrections, other, more sophisticated methods of inclusion of long-range interactions based on e.g. nonlocal density functionals such as VdW-DF can by employed [56], however, they do not provide significant improvement of the accuracy of porous crystals structural properties description [53].

DFT-based phonon calculations in nanoporous crystals are time- and resources-consuming due to usually large number of atoms in the materials' unit cells (up to several hundred), and respectively more electrons to describe. Therefore, force field (FF) approach has also been harnessed for description of intra- and intermolecular interactions, and calculations of the forces acting on the atoms. The FF methods use analytical functions to describe all types of interactions in the systems (bond and angles deformations, as well as long-range interactions). The vibrational Metal-Organic Frameworks force field (VMOF) is specifically dedicated to study phonons in MOFs [57]. This *ab-initio* derived force field uses the MM3 Buckingham potential to describe the interactions between organic and inorganic parts of the MOFs:

$$U(r_{ij}) = \varepsilon_{ij}\left[Ae^{-B\frac{r_{ij}}{r_{ij}^0}} - C\left(\frac{r_{ij}^0}{r_{ij}}\right)^6\right],$$

where ε_{ij}, A, B, C and r_{ij}^0 are interaction parameters [57] and r_{ij} is the interatomic distance. The internal and electrostatic energy terms of VMOF are written as:

$$U = \sum_{bonds}\frac{1}{2}k_r(r-r_0)^2 + \sum_{angles}\frac{1}{2}k_\theta(\theta-\theta_0)^2 \sum_{dihedrals}\frac{1}{2}k_\psi[1-\cos(n\psi+\psi_0)] + \frac{1}{2}\sum_i\sum_j\frac{1}{4\pi\varepsilon_0}\frac{q_iq_j}{r_{ij}},$$

where the successive terms describe harmonic bonds stretching, angles and dihedral angles deformation, and electrostatic interactions, respectively. It has been shown that this force field accurately describes a large variety of properties (lattice parameters, elastic properties (elastic tensor, bulk modulus), IR spectra, phonon density of states, free energies, vibrational entropies and heat capacities) of rigid frameworks (e.g., MOF-5, IRMOF-10, MOF-650, UiO-66, UiO-67, MIL-125, MOF-74 and NOTT-300). However, to the best of our knowledge, the VMOF force field has not been applied to study phonons in flexible MOFs, for which an accurate description of low-frequency modes is necessary to correctly predict possible lattice deformations and interpret their mechanisms [29,58].

Phonons can be calculated using molecular dynamics (MD) computer simulations. In principle, this approach gives a full characterization of the system: the potential energy surface, harmonic phonon frequencies, and anharmonicity. This ensemble of information is necessary to describe the breathing systems, like MIL-53. When MD simulations were performed in the anisotropic stress isothermal (NσT) statistical ensemble, in which both the shape and size of the framework are allowed to change, the short living (<25 ps), metastable intermediate structures have been observed [11]. This result was interpreted as a progressive evolution of the system structure rather than a strict transition between two distinct states. It was also suggested that the mechanism of this transformation is stimulated by a soft mode; however, the corresponding soft mode was not identified. Theoretically, such a continuous structure evolution may occur. If it is stimulated by fluid adsorption in the structure, the host/guest interactions could induce structural host deformations. If these interactions are strong enough, they can modify the character of the transformation, from the strongly discontinuous into more progressive, and/or induced by phonon soft mode. This mechanism of structural transformations has not yet received enough attention in studies of flexible microporous materials.

Collective vibrations with impact on the flexibility

Gate opening and breathing

Low frequency phonons (below 100 cm^{-1}) are unique signatures of the lattice transformation, because they gather information from all atoms. Therefore, such terahertz vibrations may be successfully used in detailed analysis of phenomena responsible for lattice flexibility.

Flexibility of metal-organic frameworks can be divided into several main categories: (i) gate-opening, (ii) breathing, (iii) negative thermal expansion. Gate-opening is coherent out-of-plane movement of organic linkers, whereas breathing phenomena represent structural lattice transformations that causes reversible yet hysteretic changes of the framework volume. There exists also simple swelling, and intra-framework dynamics (see [23])

ZIFs exhibit variety of flexible behaviors. Low elastic moduli (1-10 GPa, [59]) causes their high sensibility to deformation (in contrast with e.g. zeolites that are very rigid elastic moduli of 10-100 GPa [60]). Ryder *et al.* showed that the gate-opening observed in ZIF-4, ZIF-7 and ZIF-8 is due to the unique vibrational modes appearing in these materials [58]. In ZIF-4, two modes at about 1 THz (gate-opening) and 0.2 THz (shearing of the 4-member ring) have been identified as responsible for abnormal shape of the N_2 adsorption isotherm [61]. In ZIF-7, the vibration at 0.654 THz appearing in calculation of phonon spectra of the dried structure has been associated with experimentally observed solvent removal from the material. The modes appearing at 0.654 THz,

1.47 THz, 2.01 THz and 4.61 THz were attributed to the breathing and gate-opening framework deformations.

For ZIF-8, a coupling of the DFT simulations and inelastic neutron scattering (INS) spectroscopy allowed to explain material lattice dynamics, and to identify phonon modes responsible for structure flexibility. Similarly, as in ZIF-4, a strong mode at around 1 THz was attributed to a twisting of organic ligands and opening of the pore aperture. *In-situ* INS experiment confirmed that N_2 adsorption in ZIF-8 is possible because of swinging movement of 2-methylimidazole linkers causing gate-opening [62]. The free-swinging movement in the empty framework occurs because of weak interactions between the methyl groups of the linker. When N_2 is adsorbed in the system pores, the interactions between the linkers and the guest molecules and additional steric barriers prohibit the free swing of imidazolate linkers. The difference between calculated and experimental INS spectra is noticeable in the lowest energy region only (below 5 THz). This observation promoted the interest in applying the phonon formalism to interpret adsorption-induced structural transformations of porous flexible frameworks. A variety of ZIF type compounds with SOD topology were analyzed by Formalik *et al.* [29]. Using DFT methodology the authors calculated the IR spectra of ZIF-8, ZIF-8_amino and SALEM-2 lattices. These ZIFs have methyl group, amino group and hydrogen connected to the imidazole linker, respectively. The main deformation-related phonons modes varied with the chemical composition of the linker. A shift of the asymmetric gate-opening (IR-active mode) mode from 67 cm^{-1} (ZIF-8) through 58 cm^{-1} (ZIF-8_amino) to 37 cm^{-1} (SALEM-2) was observed, and related to the decreasing of the linker mass and increasing strength of the intramolecular interactions (mainly dispersion) between the groups connected to the imidazolate linker in the 4-member ring. The breathing modes of the 6-member ring were also identified. Furthermore, the calculations provided the IR spectrum for ZIF-8_amino which has not been synthesized yet, showing the potential of phonon spectra analysis in materials design.

The mechanism of breathing in MIL-53(Al) was analyzed using far- and mid-IR spectroscopy and DFT simulations [63]. Excellent agreement was found between the calculated and experimental spectra. A very detailed investigation of the modes impacting the breathing deformation in both stable phases of the material (large pore (LP) and closed pore (CP) structures) identified 12 and 7 low frequency modes (below 100 cm^{-1}) in LP and CP phases, respectively (excluding the acoustic modes). In both phases the lowest frequencies modes (11 cm^{-1} for CP and 15 cm^{-1} for LP phase) correspond to the metallic center rocking-like motion coupled to the slight trampoline-like motion of the organic likers. For the LP phase, the main phonon modes are located at 47 cm^{-1} (total linker rotation with alternating metallic center rotation), 54 cm^{-1} (linker rotation with different out-of-plane amplitude), 59 cm^{-1} and 60 cm^{-1} (a trampoline-like motion of linkers). Some modes above 100 cm^{-1} are also able to trigger breathing transition: the mode at 181 cm^{-1} in the LP structure (combination of scissoring motion of the metallic center and seesaw motion of the linker), and complex breathing mode located at 123 cm^{-1} in the NP structure (linker translation along the pore channel plus trampoline-like motion and additional metal octahedra rotation, Fig.

1). All principal low-frequency phonons associated with gate-opening and breathing in discussed structures are gathered in Table 1.

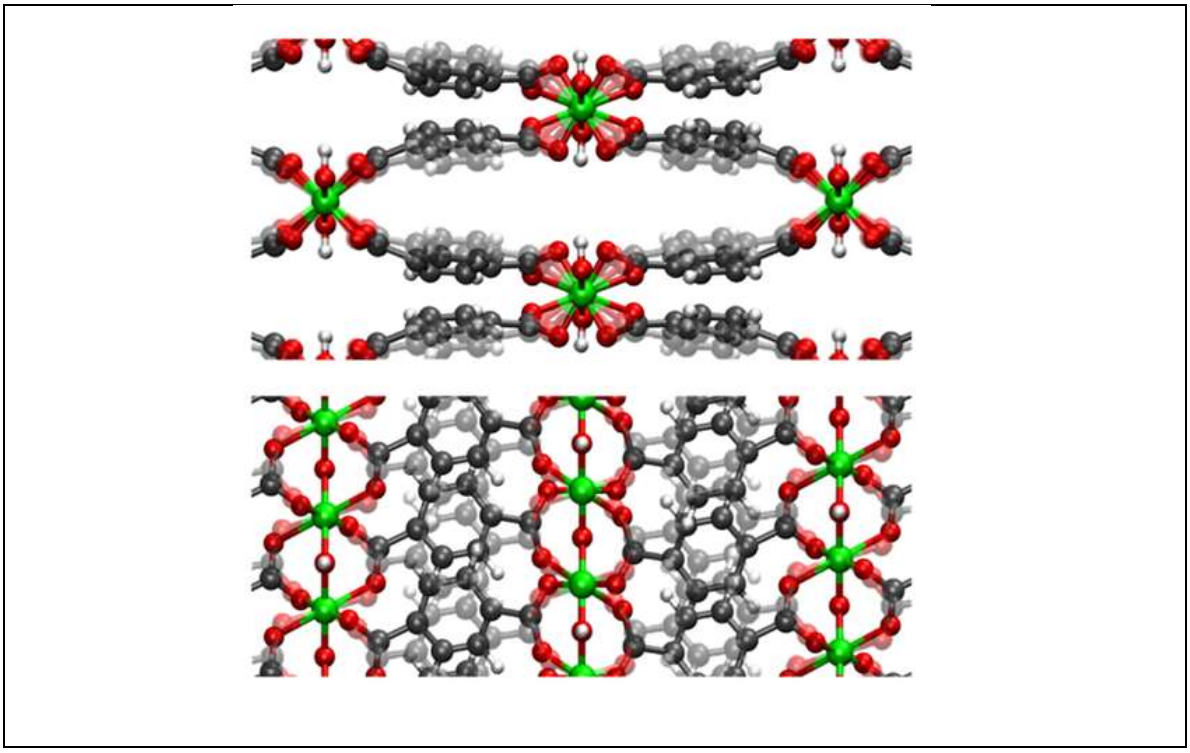

Figure 1. MIL-53(Al) breathing mode located at 123 cm^{-1}: trampoline-like organic ligand motion (top), linker translation coupled with metallic center rotation (bottom). Reprinted with permission from Ref. [63].

In the case of MIL-53(Cr) quasi-harmonic approximation was used to compute the total, Helmholtz and Gibbs free energies at different temperatures and pressures [64]. While calculating phonons the most unstable mode for LP was one responsible for hydrogen from hydroxyl group in the metallic center, whereas for NP no unstable modes were found. The calculated energy profiles between the narrow pore (NP) and large pore (LP) form are surprisingly flat. The energy of activation of structural transformation (from NP to LP phase) of 3-6 kJ per mole of $Cr_4(OH)_4(C_8H_4O_4)_4$ has been found. The two structures are almost equienergetic, the numbers vary between different density functionals used. all tested density functionals had the dispersion correction included and one with the best agreement to experimental data is meta-GGA-D3(BJ). As reported by Cockayne the relatively shallow Gibbs free energy profiles mean that even small change in pressure can shift the potential energy surface into a single minima function. In UiO-67 and IRMOF-10 the change of the dihedral angle in biphenyl-4,4-dicarboxylate (BPDC) linker caused by the large thermal displacement has been analyzed using a combination of *ab initio* Molecular Dynamics and DFT phonon calculations [65]. Imaginary harmonic modes due to the anharmonic nature of the organic linker rotation have been observed. These imaginary vibrations have been eliminated when the eigenvectors were applied in search of the properly optimized structure.

Negative thermal expansion in microporous materials

MOF-5 (also called IRMOF-1 – isorecticular MOF) is one of most widely studied hybrid nanoporous materials [66]. It is built of 1,4-benzenedicaboxylate (BDC) octahedrally coordinating ZnO_4 cluster. It has been shown both experimentally (by X-ray diffraction) and using molecular dynamics (MD) simulations that this framework exhibits a large negative-thermal expansion (NTE) [67,68], causing shrinking of lattice parameter from $25.97\ \text{Å}$ (at $26\ \text{K}$) to $25.65\ \text{Å}$ (at $700\ \text{K}$). However, neither X-ray data nor MD computational experiment could explain at the microscopic level such phenomenon. Using neutron powder diffraction and DFT calculations within quasi-harmonic approximation Zhou *et al*. showed that linear thermal expansion coefficient of IRMOF-1 is in the range between $-16 \cdot 10^6 \frac{1}{K}$ and $-10 \cdot 10^6 \frac{1}{K}$ [69]. The experimental results agree with simulations in the limits of error associated with the used functional (LDA or GGA). The NTE usually finds its origin in: (i) phase transitions, (ii) vibrations of bridging atoms, or (iii) magnetic and electric effects [70]. In the case of MOF-5, the lattice contraction model supposes that linkers of aromatic rings can be considered as associated with rotation of aromatic ring, and transverse vibration of carboxylate group of the linker which showed softening with increasing temperature. The most intense, and potentially responsible for NTE modes are transverse trampoline-like vibrations of aromatic rings, both in-phase (with frequency 18.55 cm^{-1}) and out-of-phase (at 62.91 cm^{-1} and 98.4 cm^{-1}) (Fig. 2). These vibrations effectively reduce the distance between metallic clusters and, in consequence, the lattice parameters.

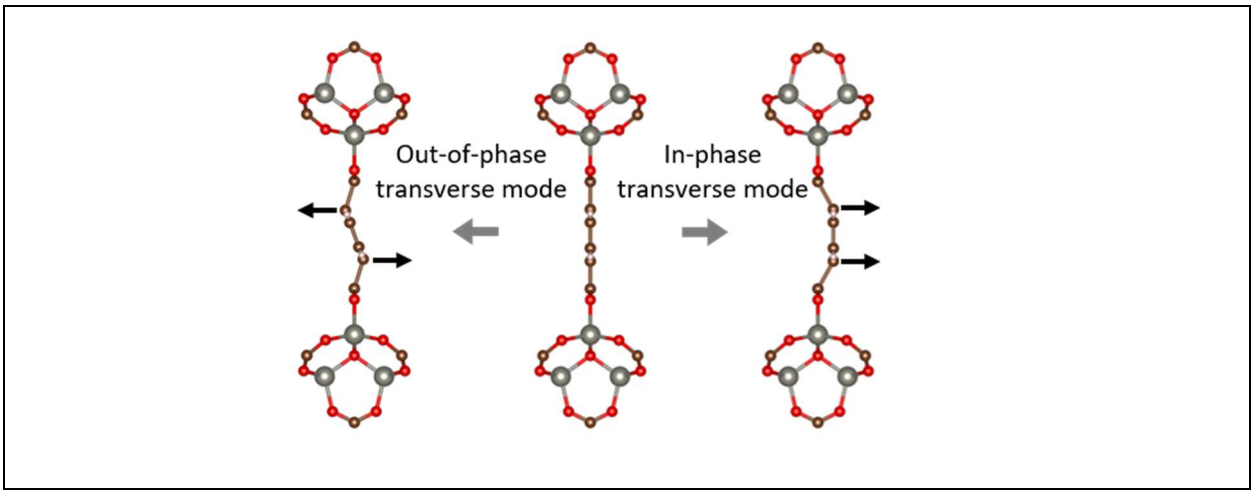

Figure 2. Trampoline-like vibrations modes of the linkers' aromatic rings in MOF-5.

NTE in MOF-5 was also analyzed by Lock *et al*. [71]. The authors interpreted neutron diffraction spectrum using Gaussian-based DFT calculations and showed that the distance between in-ring carbon atoms connected to carboxylate groups does not vary significantly with temperature, whereas distance between ring carbons and carboxylate carbon decreases with temperature.

That shows that only the in-phase mode effectively shortens the linker, and, when associated with small anharmonic thermal expansion of the bonds, leads to macroscopically observed negative thermal expansion of the structure. Additionally, as the bonds connecting carboxylates with zinc atoms within metallic cluster shorten with temperature, the rotation of metallic clusters may also contribute to this phenomenon. The nature of the linker plays a key role in framework flexibility: in CuBTC framework, formed with tricarboxylates linkers, the thermal expansion coefficient is much lower. Obviously, the 1-dimensional linkers of MOF-5 (dicarboxylate) are much easier to bend that triply-connected 2-dimensional linkers of CuBTC (tricarboxylate).

Rimmer *et al.* [72] proposed another interpretation of NTE phenomenon in MOFs. The authors showed that analysis of only optic modes at Γ-point of BZ may not provide full insight onto the NTE mechanism. In fact, when NTE is discussed, most studies tend to neglect the contributions from acoustic phonons, partially because of difficulties in measuring them experimentally. Therefore, the authors sampled the whole BZ. They mapped the calculated phonon dispersion on the individual Grüneisen parameters $\gamma_{i,\mathbf{q}}$ for each mode i with wavevector $\mathbf{q}$:

$$\gamma_{i,\mathbf{q}} = -\frac{\partial \ln \omega_{i,\mathbf{q}}}{\partial \ln V},$$

ω is the frequency of i-th mode at $\mathbf{q}$, and V is the volume of the cell. The obtained results are shown on Fig. 3 (top panel). Apart from previously reported optic modes related to transverse vibrations of linker, acoustic modes on Γ-X-W path also provide significant contribution to contraction of the unit cell length with increasing temperature. Fig. 3 (bottom panel) depicts the acoustic phonon at X-point. Upon deformation induced by this mode the effective lattice parameter shortens with respect to the initial structure. The *ab-inito* results were also correlated with those obtained using rigid unit models (RUMs), which approximate the crystal structure by describing individual groups of atoms as separate entities. Two types of cluster RUMs were proposed for MOF-5: (i) containing metallic clusters (one for totally rigid 4(ZnO_4) cluster, and one for four independent ZnO_4 tetrahedra), and (ii) containing organic linkers. Correlation of two models provided information about the types of vibrations involved in NTE. It has been shown that, in general, RUMs are sufficient to describe NTE in MOF-5, and that this phenomenon is trigged by distortion of the material on joints between separate parts of MOF, such as aromatic rings, carboxylate groups and metal clusters.

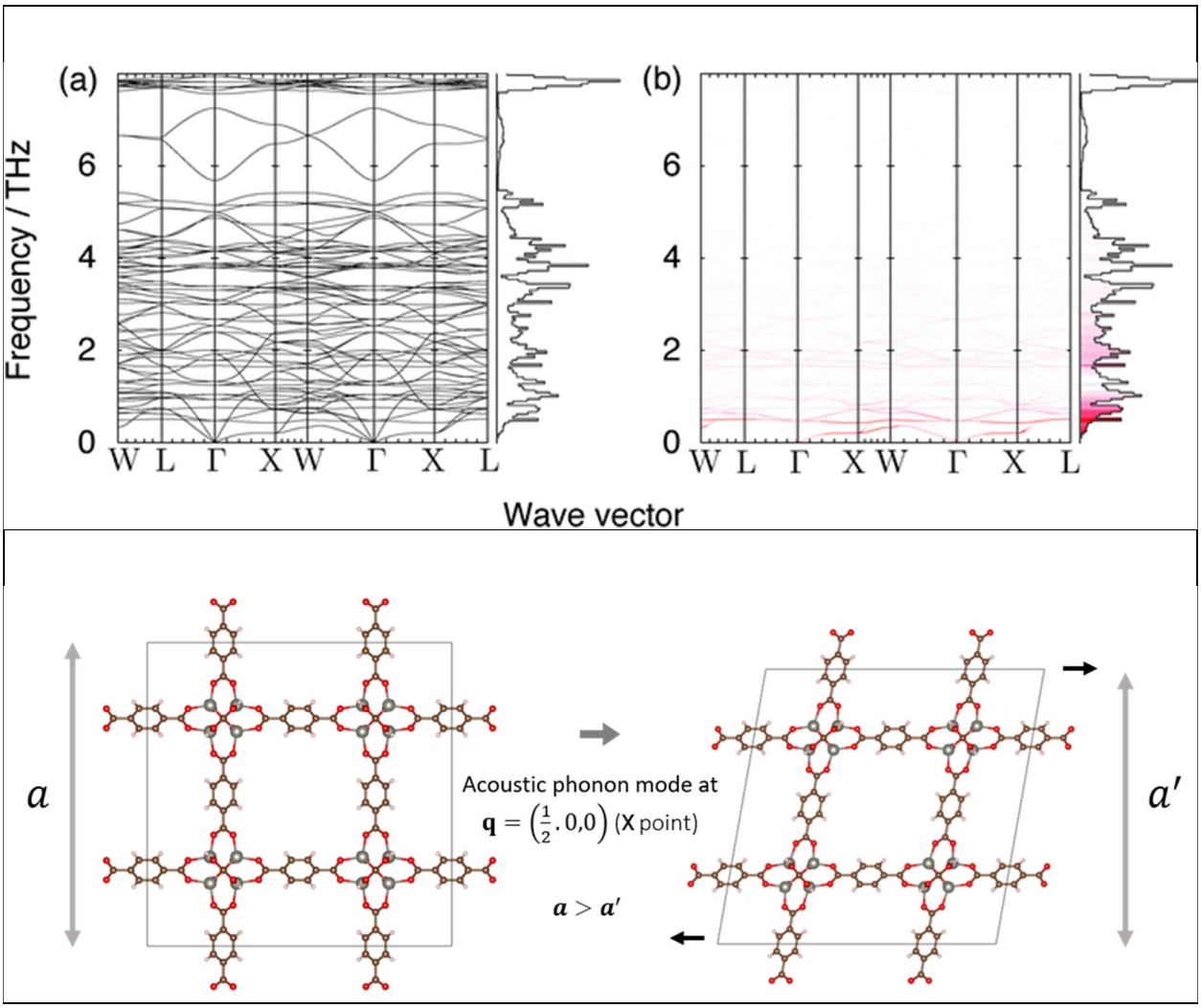

Figure 3. Top: (left) phonon dispersion and (right) colored phonon dispersion; where intensity of color represents the value of Grüneisen parameters $\gamma_{i,q}$, from red ($\gamma_{i,q} \leq -40$) to white ($\gamma_{i,q} = 0$). Bottom: deformation related to the acoustic phonon in X-point of BZ in MOF-5. Reprinted with permission from Ref. [72].

A detailed analysis of vibrational properties of CuBTC, based on IR and Raman experiments and, supported by DFT calculations was performed by Ryder *et al*. [73]. 81 modes with frequencies lower than 600 cm^{-1} were identified. Modes with frequencies higher than $100\ cm^{-1}$ were associated with bonds stretching, angles bending and deformations of both the organic linkers and the metal clusters. Framework vibrations appearing at lower frequencies include trampoline-like motions (similar to that observed in MOF-5), and rotor-like motion of the paddle-wheel clusters. All principal low-frequency phonons associated with NTE in discussed structures are gathered in Tab. 1.

Table 1. Principal modes associated with framework flexibility in IRMOF-1, HKUST-1, ZIF-4, ZIF-7, ZIF-8, SALEM-2, ZIF-7_amino and MIL-53(Al). 6MR and 4MR denotes 4-member ring and 6-member ring respectively.

Material	Frequency		Type	Description	Ref.
	cm^{-1}	THz			
IRMOF-1	19	0.57	optical	In-phase transverse, trampoline-like vibration of the linker	[69]
	63	1.89	optical	Out-of-phase transverse, trampoline-like vibration of the linker with rotation	
	98	2.94	optical	Out-of-phase transverse, trampoline-like vibration of the linker	
	7	0.21	acoustic	Acoustic mode at X-point	[72]
	10	0.30		Acoustic mode at Γ-point	
IRMOF-1 (cluster model)	32	0.96	local	In-phase transverse, trampoline-like vibration of the linker	[71]
	44	1.32		Out-of-phase transverse, trampoline-like vibration of the linker with rotation	
HKUST-1	81	2.43	optical	Transverse vibration of organic linker	[73]
	94	2.82			
	98	2.94			
	63	1.89		Paddle-wheel deformation	
	78	2.34			
	16	0.48			
	20	0.60			
	58	1.74			
ZIF-4	7	0.20	optical	Soft mode of 4MR	[58]
	33	1.00		Gate-opening of 6MR	
ZIF-7	22	0.65		Soft mode of 6MR	
	2	0.06		Breathing of 6MR and shearing of 4MR	
	49	1.47		Breathing of 6MR	
ZIF-8	19	0.57		Soft mode of 6MR	
	33	1.00		Gate-opening of 4MR	
ZIF-8	40	1.20	optical	Symmetric gate-opening of 4MR	[29]
	67	2.01		Asymmetric gate-opening of 4MR	
	100	3.00		Breathing of 6MR	
SALEM-2	43	1.29		Symmetric gate-opening of 4MR	
	37	1.11		Asymmetric gate-opening of 4MR	
	105	3.15		Breathing of 6MR	
ZIF-8_amino	50	1.50		Symmetric gate-opening of 4MR	
	58	1.74		Asymmetric gate-opening of 4MR	
	97	2.91		Breathing of 6MR	

MIL-53(Al) CP	11	0.33	optical	The metallic center rocking-like motion coupled to slight trampoline-like motion of the organic likers	[63]
	123	3.69		Linker translation along the pore channel plus trampoline-like motion and additional metal octahedra rotation	
MIL-53(Al) LP	15	0.45	optical	The metallic center rocking-like motion coupled to slight trampoline-like motion of the organic likers	
	47	1.41		Total linker rotation with alternating metallic center rotation	
	54	1.62		Linker rotation	
	59	1.77		Trampoline-like motion of linkers	
	181	5.43		Combination of scissoring motion of the metallic center and seesaw motion of the linker	

Discussion and Conclusions

Mechanical fluctuations existing in the crystalline solids at equilibrium conditions may be fully characterized using phonon formalism. Phonons constitute the microscopic basis of macroscopic properties of any flexible system. In the case of the second order structural phase transformation phonons constitute the first indicators of system evolution towards instabilities. They are called the soft modes when their frequency tends to zero at the instability point. As related to the phase transformations in microporous crystalline solids, the existence of the soft modes may be associated with the limits of phase metastability corresponding to the transition from the elastic to plastic deformation. The calculation of soft modes is the numerical tool which can provide supplementary information about the mechanism of deformations observed in microporous materials.

However, the phonon modes represent only the harmonic part of the potential energy surface (PES). Amplitudes of atomic displacement in harmonic approximation are very small, to preserve the system in the harmonic region. They cannot predict the mechanism of the transformation if a large variation of atomic positions is involved. In such situation, the anharmonic analysis must be performed, followed by a detailed analysis of PES.

A new non-perturbative approach to anharmonicity using Hellman-Feynman forces was recently proposed by Parlinski [37]. Anharmonic modes are temperature-dependent and amplitudes of vibration become functions of temperature. Their frequencies can be shifted with respect to the harmonic value. Also, their spectral distribution cannot be any longer represented by δ functions but by peaks with finite width (Gaussians peaks). The resulting phonon (dispersion) curves are

represented by phonon band depending on the Gaussians peaks width. The anharmonic corrections can modify the soft mode behavior, in two ways: either making them softer or stabilizing them.

In the case of large volume changes leading to first order structural transformations, the quasi-harmonic approach is used. In this approximation, anharmonic dependence of energy on volume is approximated by set of separate, fixed-volume calculations within harmonic approximation. It allows to take anharmonic contribution implicitly into account, and hence study properties of crystals such as free energy (F) or free enthalpy (G) to study behaviour of energy vs. volume curve with respect to changes in temperature, external pressure or adsorption stress induced by guest molecules confined in porous crystals. From the set of $F(V)$ curves for a particular temperature range it is possible to evaluate thermal expansion coefficient as:

$$\beta(T) = \frac{1}{V(T)} \frac{\partial V(T)}{\partial T}.$$

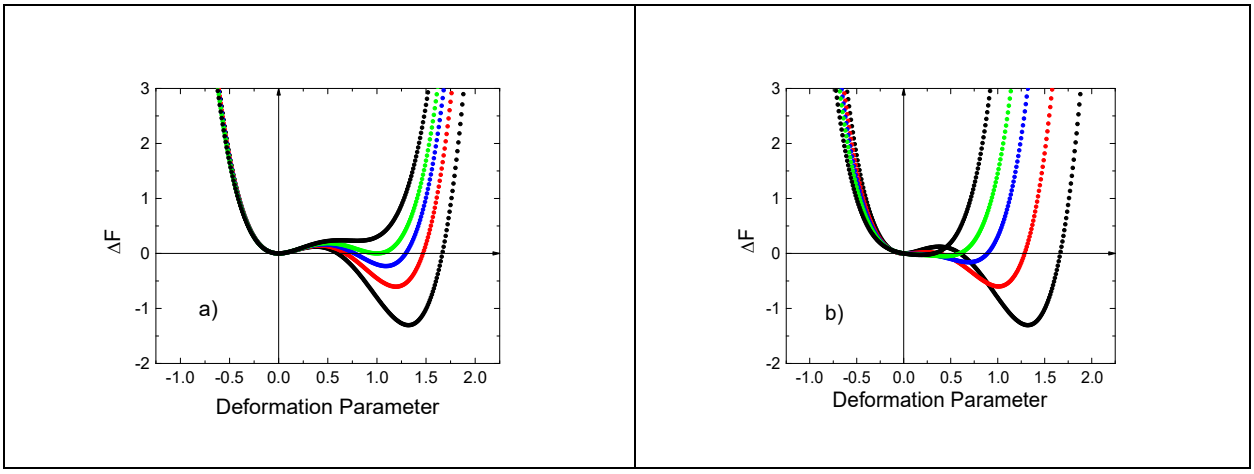

Figure 4. Free energy evolution during a first order structural transformation. The *Deformation parameter* indicates any order parameter (OP) which transforms from OP=0 (not deformed phase) into OP≠0 (deformed phase). a) Typical ΔF (OP) dependence, stimulated by the variation of the temperature or pressure (different colors correspond to different temperatures or pressures, respectively); the green curve represents the situation when both (deformed and not deformed) phases are in equilibrium (two minima with the same energy)), upper black curve corresponds to the metastability limit of the deformed phase (spinodal) b) hypothetical ΔF evolution rescaled by the adsorption, all curves have only one global minimum. If two minima exist, they have always different energy (different colors represent the free energy of the system with different adsorption uptake)

A similar quasi-harmonic approach can be proposed in the case of the deformation of flexible porous sorbents. The evolution of the phonon energies during adsorption-induced structure deformation can be approximated by set of separate, fixed-uptake calculations within harmonic approximation. The increasing guest-host interaction may renormalize the phonon spectrum. In the case of strong interactions, it may hypothetically change the character of the structure

transformation, e.g. it may stabilize the intermediate structures, and modify the free energy profile. In the limiting case, the interaction with adsorbing molecules could transform the discontinuous, thermodynamically non-reversible transformation (Fig. 4a) of the microporous empty framework into reversible continuous deformation between deformed and non-deformed states (Fig. 4b). All intermediate state are in equilibrium, stabilized by the adsorption uptake. A methodology for phonon calculations in such situation does not exist and must be developed.

Acknowledgements

BK, FF and JR acknowledge support from the Polish National Science Center (NCN, grant no. 2015/17/B/ST8/00099)

References

[1] M. Born, K. Huang, Dynamical Theory of Crystal Lattice, Oxford University Press, 1954.

[2] S. Kitagawa, K. Uemura, Dynamic porous properties of coordination polymers inspired by hydrogen bonds, Chem. Soc. Rev. 34 (2005) 109–119. doi:10.1039/b313997m.

[3] S. Horike, S. Shimomura, S. Kitagawa, Soft porous crystals, Nat. Chem. 1 (2009) 695–704. doi:10.1038/nchem.444.

[4] G. Férey, C. Serre, Large breathing effects in three-dimensional porous hybrid matter: Facts, analyses, rules and consequences, Chem. Soc. Rev. 38 (2009) 1380–1399. doi:10.1039/b804302g.

[5] M. Alhamami, H. Doan, C.H. Cheng, A review on breathing behaviors of metal-organic-frameworks (MOFs) for gas adsorption, Materials (Basel). 7 (2014) 3198–3250. doi:10.3390/ma7043198.

[6] J. Wieme, L. Vanduyfhuys, S.M.J. Rogge, M. Waroquier, V. Van Speybroeck, Exploring the flexibility of MIL-47(V)-type materials using force field molecular dynamics simulations, J. Phys. Chem. C. 120 (2016) 14934–14947. doi:10.1021/acs.jpcc.6b04422.

[7] A.U. Ortiz, A. Boutin, A.H. Fuchs, F.X. Coudert, Investigating the pressure-induced amorphization of zeolitic imidazolate framework ZIF-8: Mechanical instability due to shear mode softening, J. Phys. Chem. Lett. 4 (2013) 1861–1865. doi:10.1021/jz400880p.

[8] A. Phan, C.J. Doonan, F.J. Uribe-Romo, C.B. Knobler, M. O'Keeffe, O.M. Yaghi, Synthesis, Structure, and Carbon Dioxide Capture Properties of Zeolitic Imidazolate Frameworks, Acc. Chem. Res. xxx (2009).

[9] A. Schneemann, V. Bon, I. Schwedler, I. Senkovska, S. Kaskel, R.A. Fischer, Flexible metal-organic frameworks, Chem. Soc. Rev. 43 (2014) 6062–6096. doi:10.1039/c4cs00101j.

[10] C.R. Murdock, B.C. Hughes, Z. Lu, D.M. Jenkins, Approaches for synthesizing breathing MOFs by exploiting dimensional rigidity, Coord. Chem. Rev. 258–259 (2014) 119–136. doi:10.1016/j.ccr.2013.09.006.

[11] A. Ghoufi, G. Maurin, G. Férey, Physics behind the guest-assisted structural transitions of a porous metal-organic framework material, J. Phys. Chem. Lett. 1 (2010) 2810–2815. doi:10.1021/jz1011274.

[12] A. Ghoufi, K. Benhamed, L. Boukli-Hacene, G. Maurin, Electrically Induced Breathing of the MIL-53(Cr) Metal-Organic Framework, ACS Cent. Sci. 3 (2017) 394–398. doi:10.1021/acscentsci.6b00392.

[13] Y. Liu, J. Her, A. Dailly, A.J. Ramirez-cuesta, Reversible Structural Transition in MIL-53 with Large Temperature Hysteresis, (2008) 11813–11818.

[14] I. Beurroies, M. Boulhout, P.L. Llewellyn, B. Kuchta, G. Férey, C. Serre, R. Denoyel, Using pressure to provoke the structural transition of metal-organic frameworks, Angew. Chemie - Int. Ed. 49 (2010) 7526–7529. doi:10.1002/anie.201003048.

[15] D. Fairen-Jimenez, S.A. Moggach, M.T. Wharmby, P.A. Wright, S. Parsons, T. Düren, Opening the gate: Framework flexibility in ZIF-8 explored by experiments and simulations, J. Am. Chem. Soc. 133 (2011) 8900–8902. doi:10.1021/ja202154j.

[16] T. Loiseau, C. Serre, C. Huguenard, G. Fink, F. Taulelle, M. Henry, T. Bataille, G. Férey, A Rationale for the Large Breathing of the Porous Aluminum Terephthalate (MIL-53) Upon Hydration, Chem. - A Eur. J. 10 (2004) 1373–1382. doi:10.1002/chem.200305413.

[17] F. Millange, N. Guillou, R.I. Walton, J.M. Grenèche, I. Margiolaki, G. Férey, Effect of the nature of the metal on the breathing steps in MOFs with dynamic frameworks, Chem. Commun. (2008) 4732–4734. doi:10.1039/b809419e.

[18] C. Serre, F. Millange, C. Thouvenot, M. Noguès, G. Marsolier, D. Louër, G. Férey, Very large breathing effect in the first nanoporous chromium(III)-based solids: MIL-53 or CrIII(OH)·{O2C-C6H4- CO2}·{HO2C-C6H4 -CO2H}x·H2Oy, J. Am. Chem. Soc. 124 (2002) 13519–13526. doi:10.1021/ja0276974.

[19] S. Bourrelly, P.L. Llewellyn, C. Serre, F. Millange, T. Loiseau, G. Férey, Different adsorption behaviors of methane and carbon dioxide in the isotypic nanoporous metal terephthalates MIL-53 and MIL-47, J. Am. Chem. Soc. 127 (2005) 13519–13521. doi:10.1021/ja054668v.

[20] J.D. Evans, L. Bocquet, F.X. Coudert, Origins of Negative Gas Adsorption, Chem. 1 (2016) 873–886. doi:10.1016/j.chempr.2016.11.004.

[21] D. Bousquet, F.X. Coudert, A.G.J. Fossati, A. V. Neimark, A.H. Fuchs, A. Boutin, Adsorption induced transitions in soft porous crystals: An osmotic potential approach to multistability and intermediate structures, J. Chem. Phys. 138 (2013). doi:10.1063/1.4802888.

[22] S. Krause, V. Bon, I. Senkovska, U. Stoeck, D. Wallacher, D.M. Többens, S. Zander, R.S. Pillai, G. Maurin, F.X. Coudert, S. Kaskel, A pressure-amplifying framework material with negative gas adsorption transitions, Nature. 532 (2016) 348–352. doi:10.1038/nature17430.

[23] F.X. Coudert, A. Boutin, A.H. Fuchs, A. V Neimark, Adsorption Deformation and Structural Transitions in Metal − Organic Frameworks: From the Unit Cell to the Crystal, J. Phys. Chem. Lett. 4 (2013) 3198. doi:10.1021/jz4013849.

[24] U. Stoeck, S. Krause, V. Bon, I. Senkovska, S. Kaskel, A highly porous metal-organic framework, constructed from a cuboctahedral super-molecular building block, with exceptionally high methane uptake, Chem. Commun. 48 (2012) 10841–10843. doi:10.1039/c2cc34840c.

[25] D. Li, K. Kaneko, Hydrogen bond-regulated microporous nature of copper complex-assembled microcrystals, Chem. Phys. Lett. 335 (2001) 50–56. doi:10.1016/S0009-2614(00)01419-6.

[26] P.A. Fleury, The Effects of Soft Modes on the Structure and Properties of Materials, Annu. Rev. Mater. Sci. 6 (1976) 157–180.

[27] B. Kuchta, T. Luty, R.J. Meier, The α-β phase transition in solid oxygen, J. Phys. C Solid State Phys. 20 (1987) 585–599. doi:10.1088/0022-3719/20/4/009.

[28] B. Kuchta, T. Luty, Lattice dynamics of solid nitrogen with an ab initio intermolecular potential. II. Anharmonic librations in the α phase, J. Chem. Phys. 78 (1983) 1447–1452. doi:10.1063/1.444887.

[29] F. Formalik, M. Fischer, J. Rogacka, L. Firlej, B. Kuchta, Effect of low frequency phonons on structural properties of ZIFs with SOD topology, Microporous Mesoporous Mater. (2018) 0–1. doi:10.1016/j.micromeso.2018.09.033.

[30] P.L. Llewellyn, G. Maurin, T. Devic, S. Loera-Serna, N. Rosenbach, C. Serre, S. Bourrelly, P. Horcajada, Y. Filinchuk, G. Férey, Prediction of the conditions for breathing of metal organic framework materials using a combination of X-ray powder diffraction, microcalorimetry, and molecular simulation, J. Am. Chem. Soc. 130 (2008) 12808–12814. doi:10.1021/ja803899q.

[31] C. Serre, S. Bourrelly, A. Vimont, N.A. Ramsahye, G. Maurin, P.L. Llewellyn, M. Daturi, Y. Filinchuk, O. Leynaud, P. Barnes, G. Férey, An explanation for the very large breathing effect of a metal-organic framework during CO2adsorption, Adv. Mater. 19 (2007) 2246–2251. doi:10.1002/adma.200602645.

[32] A. V. Neimark, F.X. Coudert, A. Boutin, A.H. Fuchs, Stress-based model for the breathing of metal-organic frameworks, J. Phys. Chem. Lett. 1 (2010) 445–449. doi:10.1021/jz9003087.

[33] C. Triguero, F.X. Coudert, A. Boutin, A.H. Fuchs, A. V. Neimark, Mechanism of breathing transitions in metal-organic frameworks, J. Phys. Chem. Lett. 2 (2011) 2033–2037. doi:10.1021/jz2008769.

[34] P. Hohenberg, W. Kohn, Inhomogeneous Electron Gas, Phys. Rev. 136 (1964) B864. doi:10.1103/PhysRevB.7.1912.

[35] W. Kohn, L.J. Sham, Self-Consistent Equations Including Exchange and Coorelation Effects, Phys. Rev. 385 (1965). doi:http://dx.doi.org/10.1103/PhysRev.140.A1133.

[36] R.P. Feynman, Forces in molecules, Phys. Rev. 56 (1939) 340–343. doi:10.1103/PhysRev.56.340.

[37] K. Parlinski, Ab initio determination of anharmonic phonon peaks, Phys. Rev. B. 98 (2018) 1–11. doi:10.1103/PhysRevB.98.054305.

[38] A. Togo, I. Tanaka, First principles phonon calculations in materials science, Scr. Mater. 108 (2015) 1–5. doi:10.1016/j.scriptamat.2015.07.021.

[39] K. Parlinski, Z.Q. Li, Y. Kawazoe, First-principles determination of the soft mode in cubic ZrO2, Phys. Rev. Lett. 78 (1997) 4063–4066. doi:10.1103/PhysRevLett.78.4063.

[40] K. Parlinski, Calculation of phonon dispersion curves by the direct method, 479 (1999) 121–126. doi:10.1063/1.59457.

[41] G. Kresse, J. Hafner, Ab initio molecular dynamics for liquid metals, Phys. Rev. B. 47 (1993) 558–561. doi:10.1103/PhysRevB.47.558.

[42] G. Kresse, J. Furthmuller, Efficient iterative schemes for ab initio total-energy calculations using a plane-wave basis set, Phys. Rev. B. 54 (1996) 11169–11186. doi:10.1103/PhysRevB.54.11169.

[43] G. Kresse, D. Joubert, From ultrasoft pseudopotentials to the projector augmented-wave method, Phys. Rev. B. 59 (1999) 1758–1775. doi:10.1103/PhysRevB.59.1758.

[44] S.J. Clark, M.D. Segall, C.J. Pickard, P.J. Hasnip, M.I.J. Probert, K. Refson, M.C. Payne, First principles methods using CASTEP, Zeitschrift Für Krist. 220 (2005) 567–570. doi:10.1524/zkri.220.5.567.65075.

[45] P. Giannozzi, S. Baroni, N. Bonini, M. Calandra, R. Car, C. Cavazzoni, D. Ceresoli, G.L. Chiarotti, M. Cococcioni, I. Dabo, A. Dal Corso, S. De Gironcoli, S. Fabris, G. Fratesi, R. Gebauer, U. Gerstmann, C. Gougoussis, A. Kokalj, M. Lazzeri, L. Martin-Samos, N. Marzari, F. Mauri, R. Mazzarello, S. Paolini, A. Pasquarello, L. Paulatto, C. Sbraccia, S. Scandolo, G. Sclauzero, A.P. Seitsonen, A. Smogunov, P. Umari, R.M. Wentzcovitch, QUANTUM ESPRESSO: A modular and open-source software project for quantum simulations of materials, J. Phys. Condens. Matter. 21 (2009). doi:10.1088/0953-8984/21/39/395502.

[46] R. Dovesi, A. Erba, R. Orlando, C.M. Zicovich-Wilson, B. Civalleri, L. Maschio, M. Rérat, S. Casassa, J. Baima, S. Salustro, B. Kirtman, Quantum-mechanical condensed matter simulations with CRYSTAL, Wiley Interdiscip. Rev. Comput. Mol. Sci. 8 (2018) 1–36. doi:10.1002/wcms.1360.

[47] X. Gonze, Perturbation expansion of variational principles at arbitrary order, Phys. Rev. A. 52 (1995) 1086–1095. doi:10.1103/PhysRevA.52.1086.

[48] S. Baroni, P. Giannozzi, A. Testa, Greens-function approach to linear response in solids,

Phys. Rev. Lett. 58 (1987) 1861–1864. doi:10.1103/PhysRevLett.58.1861.

[49] M. Fischer, Structure and bonding of water molecules in zeolite hosts: Benchmarking plane-wave DFT against crystal structure data, Zeitschrift Fur Krist. - Cryst. Mater. 230 (2015) 325–336. doi:10.1515/zkri-2014-1809.

[50] M. Fischer, F.O. Evers, F. Formalik, A. Olejniczak, Benchmarking DFT-GGA calculations for the structure optimisation of neutral-framework zeotypes, Theor. Chem. Acc. 135 (2016) 1–19. doi:10.1007/s00214-016-2014-6.

[51] M. Fischer, R.J. Angel, Accurate structures and energetics of neutral-framework zeotypes from dispersion-corrected DFT calculations, J. Chem. Phys. 146 (2017). doi:10.1063/1.4981528.

[52] F. Formalik, M. Fischer, J. Rogacka, L. Firlej, B. Kuchta, Benchmarking of GGA density functionals for modeling structures of nanoporous, rigid and flexible MOFs, J. Chem. Phys. 149 (2018). doi:10.1063/1.5030493.

[53] D. Nazarian, P. Ganesh, D.S. Sholl, Benchmarking density functional theory predictions of framework structures and properties in a chemically diverse test set of metal-organic frameworks, J. Mater. Chem. A. 3 (2015) 22432–22440. doi:10.1039/c5ta03864b.

[54] S. Grimme, Semiempirical GGA-Type Density Functional Constructed with a Long-Range Dispersion Correction, J. Comput. Chem. 27 (2006) 1787–1799. doi:10.1002/jcc.

[55] F. Formalik, M. Fischer, J. Rogacka, L. Firlej, B. Kuchta, Benchmarking of GGA density functionals for modeling structures of nanoporous, rigid and flexible MOFs, J. Chem. Phys. 149 (2018). doi:10.1063/1.5030493.

[56] K. Lee, É.D. Murray, L. Kong, B.I. Lundqvist, D.C. Langreth, Higher-accuracy van der Waals density functional, Phys. Rev. B - Condens. Matter Mater. Phys. 82 (2010) 3–6. doi:10.1103/PhysRevB.82.081101.

[57] J.K. Bristow, J.M. Skelton, K.L. Svane, A. Walsh, J.D. Gale, A general forcefield for accurate phonon properties of metal-organic frameworks, Phys. Chem. Chem. Phys. 18 (2016) 29316–29329. doi:10.1039/c6cp05106e.

[58] M.R. Ryder, B. Civalleri, T. Bennett, S. Henke, S. Rudić, G. Cinque, F. Fernandez-Alonso, J.C. Tan, Identifying the role of terahertz vibrations in metal-organic frameworks: From gate-opening phenomenon to shear-driven structural destabilization, Phys. Rev. Lett. 113 (2014) 1–6. doi:10.1103/PhysRevLett.113.215502.

[59] J.C. Tan, T.D. Bennett, A.K. Cheetham, Chemical structure, network topology, and porosity effects on the mechanical properties of Zeolitic Imidazolate Frameworks, PNAS. 107 (2010) 9938–9943. doi:10.1073/pnas.1003205107/-/DCSupplemental.www.pnas.org/cgi/doi/10.1073/pnas.1003205107.

[60] J.C. Tan, A.K. Cheetham, Mechanical properties of hybrid inorganic-organic framework materials: Establishing fundamental structure-property relationships, Chem. Soc. Rev. 40

(2011) 1059–1080. doi:10.1039/c0cs00163e.

[61] T.D. Bennett, S. Cao, J.C. Tan, D.A. Keen, E.G. Bithell, P.J. Beldon, T. Friscic, A.K. Cheetham, Facile mechanosynthesis of amorphous zeolitic imidazolate frameworks, J. Am. Chem. Soc. 133 (2011) 14546–14549. doi:10.1021/ja206082s.

[62] M.E. Casco, Y.Q. Cheng, L.L. Daemen, D. Fairen-Jimenez, E. V. Ramos-Fernández, A.J. Ramirez-Cuesta, J. Silvestre-Albero, Gate-opening effect in ZIF-8: The first experimental proof using inelastic neutron scattering, Chem. Commun. 52 (2016) 3639–3642. doi:10.1039/c5cc10222g.

[63] A.E.J. Hoffman, L. Vanduyfhuys, I. Nevjestić, J. Wieme, S.M.J. Rogge, H. Depauw, P. Van Der Voort, H. Vrielinck, V. Van Speybroeck, Elucidating the Vibrational Fingerprint of the Flexible Metal-Organic Framework MIL-53(Al) Using a Combined Experimental/Computational Approach, J. Phys. Chem. C. 122 (2018) 2734–2746. doi:10.1021/acs.jpcc.7b11031.

[64] E. Cockayne, Thermodynamics of the Flexible Metal-Organic Framework Material MIL-53(Cr) from First-Principles, J. Phys. Chem. C. 121 (2017) 4312–4317. doi:10.1021/acs.jpcc.6b11692.

[65] K.L. Svane, J.K. Bristow, A. Walsh, Anharmonic Origin of Giant Thermal Displacements in the Metal-Organic Framework UiO-67, J. Phys. Chem. C. 121 (2017) 22010–22014. doi:10.1021/acs.jpcc.7b04757.

[66] J.L.C. Rowsell, E.C. Spencer, J. Eckert, J.A.K. Howard, O.M. Yaghi, Gas Adsorption Sites in a Large-Pore Metal-Organic Framework, Science (80-.). 309 (2005) 1350–1354. doi:10.1126/science.1113247.

[67] D. Dubbeldam, K.S. Walton, D.E. Ellis, R.Q. Snurr, Exceptional Negative Thermal Expansion in Isoreticular Metal – Organic Frameworks **, (2007) 4496–4499. doi:10.1002/anie.200700218.

[68] S.S. Han, W.A. Goddard, Metal−Organic Frameworks Provide Large Negative Thermal Expansion Behavior, J. Phys. Chem. C. 111 (2007) 15185–15191. doi:10.1021/jp075389s.

[69] W. Zhou, H. Wu, T. Yildirm, J.R. Simpson, A.R. Hight Walker, Origin of the exceptional negative thermal expansion in metal-organic framework-5 Zn4O(1,4-benzenedicarboxylate)3, Phys. Rev. B. 78 (2008) 054114. doi:10.1103/PhysRevB.78.054114.

[70] J.S.O. Evans, Negative thermal expansion materials, J. Chem. Soc. Dalt. Trans. (1999) 3317–3326.

[71] N. Lock, M. Christensen, Y. Wu, V.K. Peterson, M.K. Thomsen, R.O. Piltz, A.J. Ramirez-Cuesta, G.J. McIntyre, K. Norén, R. Kutteh, C.J. Kepert, G.J. Kearley, B.B. Iversen, Scrutinizing negative thermal expansion in MOF-5 by scattering techniques and ab initio calculations, Dalt. Trans. 42 (2013) 1996–2007. doi:10.1039/C2DT31491F.

[72] L.H.N. Rimmer, M.T. Dove, A.L. Goodwin, D.C. Palmer, Acoustic phonons and negative thermal expansion in MOF-5, Phys. Chem. Chem. Phys. 16 (2014) 21144–21152. doi:10.1039/C4CP01701C.

[73] M.R. Ryder, B. Civalleri, G. Cinque, J.C. Tan, Discovering connections between terahertz vibrations and elasticity underpinning the collective dynamics of the HKUST-1 metal-organic framework, CrystEngComm. 18 (2016) 4303–4312. doi:10.1039/c5ce02347e.